High-performance algorithm to calculate spin- and parity-dependent nuclear level densities

R. A. Sen'kov and M. Horoi
Department of Physics, Central Michigan University, Mount Pleasant, Michigan 48859, USA
(Received 30 April 2010; published 3 August 2010)

A new algorithm for calculating the spin- and parity-dependent shell-model nuclear level densities using the moments method in the proton-neutron formalism is presented. A new, parallelized code based on this algorithm was developed and tested using up to 4000 cores for a set of nuclei from the sd-, pf-, and $pf + g_{9/2}$-model spaces. By comparing the nuclear level densities at low excitation energy for a given nucleus calculated in two model spaces, such as pf and $pf + g_{9/2}$, one can estimate the ground-state energy in the larger model space, which is not accessible to direct shell-model calculations due to the unmanageable dimension. Examples for the ground-state energies of for ^{64}Ge and ^{68}Se in the $pf + g_{9/2}$ model space are presented.

DOI: 10.1103/PhysRevC.82.024304 PACS number(s): 21.10.Ma, 21.10.Dr, 21.10.Hw, 21.60.Cs

I. INTRODUCTION

Spin- and parity-dependent nuclear level densities represent an important ingredient for the theory of nuclear reactions. For example, the Hauser-Feschbach approach [1] requires exact knowledge of nuclear level densities for certain quantum numbers J^π of spin and parity in the Gamow window of excitation energies around the particle threshold [2,3]. In most of the cases relevant to nuclear astrophysics, where experimental information is not available, the reaction rates for medium and heavy nuclei can only be estimated using the Hauser-Feshbach approach. Nuclear level densities are usually obtained using the back-shifted Fermi gas approximation [4–6], which was improved over the years. More modern approaches to the level densities based on the mean field were recently proposed by Goriely and collaborators [7–9]. These approximations assume an independent particle model in a mean field that lacks information about the many-body correlations. These correlations can be included exactly if one can fully diagonalize the many-body nuclear Hamiltonian, a task of increasing difficulty. Alternatively, one can use Monte-Carlo techniques [10–15], or other methods of the statistical spectroscopy [16,17], including applications to large shell-model spaces [18,19].

Most of these methods [2,10–12,20,21] calculate the *density of states* and later use a spin-weight factor that includes an energy-dependent cutoff parameter to extract the spin-dependent *nuclear level density*. Although there are recent efforts to improve the accuracy of such parametrizations [21]. It was shown that the spin cutoff parameter has very large fluctuations at low excitation energy, when compared with the shell-model results [22]. Statistical spectroscopy provides a path to a direct calculation of the spin cutoff parameter using a polynomial expansion for its estimate [23]. This approach was recently investigated (see Fig. 2 of Ref. [22]), where it was shown that although the smooth part of the energy dependence of the spin cutoff parameter can be described reasonably well, significant fluctuations are still present in the low-energy regime. The quality of the results of this approach are mixed. Therefore, one would like to have a spin-projected method of calculating nuclear level densities that is accurate and fast. The parity is usually taken as equally distributed, although there are attempts [13,24] to model the effect of the uneven parity-dependence of the level densities at the low excitation energies of interest for nuclear astrophysics.

Recently, we developed a strategy [22,25–27] of calculating the spin- and parity-dependent shell-model level density. The main ingredients are: (i) extension of methods of statistical spectroscopy [23,28] by exactly calculating the first and second moments for different configurations at fixed spin and parity; (ii) exact decomposition of many-body configurational space into classes corresponding to different parities and number of harmonic oscillator excitations; (iii) development of new effective interactions for model spaces of interest starting with the G matrix [29] and fixing/fitting monopole terms and/or linear combinations of two-body matrix elements to experimental data; and (iv) an accurate estimate of the shell model ground-state (g.s.) energy. The calculation of the latest ingredient is generally as time consuming as the previous three. One can minimize this effort using the exponential convergence method suggested and applied in Refs. [30–32], and/or the recently developed projected configuration interaction method [33,34]. In reverse, one can envision using some knowledge about the level density to extract the g.s. energy. This idea is not new (see, for example, Refs. [23,35–37]). However, we propose new algorithm that extracts the g.s. energy for a large model space by comparing the level density with that obtained in a reduced model space that can be exactly solved.

The techniques described in this article are based on nuclear statistical spectroscopy [23]. We calculate the configuration spin and parity projected moments of the nuclear shell-model Hamiltonian, which can be further used to obtain an accurate description of the nuclear level density up to about 15 MeV excitation energy. Therefore, our methodology does not require any spin-cutoff parameter. One should mention that some of the more recent Monte Carlo approaches for level densities can also use direct spin projection techniques [14].

The article is organized as follows. In Sec. II the fixed spin- and parity-dependent configuration moments method is revisited. The method allows one to trace such quantum numbers as parity and angular momentum explicitly. The extension of the algorithm to the proton-neutron formalism is discussed in Sec. III. Section IV is devoted to the results of the

moments method, which are compared to exact shell-model results and the results from Hartree-Fock-Bogoliubov plus combinatorial method. In Sec. IV we also present our new algorithm to extract the g.s. energy by comparing level density in related model spaces. Section V is devoted to conclusions and future prospects of the moments method.

II. SPIN- AND PARITY-DEPENDENT CONFIGURATION MOMENTS METHOD

In this work we closely follow the approach proposed in Refs. [25,26]. According to this approach one can calculate the nuclear level density ρ as a function of excitation energy E in the following way:

$$\rho(E,\alpha) = \sum_{\kappa} D_{\alpha\kappa} \cdot G_{\alpha\kappa}(E). \tag{1}$$

Here, $\alpha = \{n, J, T_z, \pi\}$ is a set of quantum numbers, where n is the number of particles (protons and neutrons), J is total spin, T_z is isospin projection, and π is parity. κ represents a configuration of n particles distributed over q spherical single-particle orbitals. Each configuration κ is fixed by a set of occupation numbers $\kappa = \{\kappa_1, \kappa_2, \ldots, \kappa_q\}$, where κ_j is the number of particles occupying the spherical single-particle level j. Each configuration has a certain number of particles, isospin projection, and parity. The sum in Eq. (1) spans all possible configurations corresponding to the given values of n, T_z, and π. The dimension $D_{\alpha\kappa}$ equals the number of many-body states with given J that can be built for a given configuration κ. The function $G_{\alpha\kappa}$ is a finite-range Gaussian defined as in Ref. [25]

$$G_{\alpha\kappa}(E) = G(E + E_{\rm gs} - E_{\alpha\kappa}, \sigma_{\alpha\kappa}), \tag{2}$$

$$G(x,\sigma) = N \cdot \begin{cases} \exp(-x^2/2\sigma^2), & |x| \leqslant \eta\cdot\sigma \\ 0, & |x| > \eta\cdot\sigma \end{cases}, \tag{3}$$

where $E_{\alpha\kappa}$ and $\sigma_{\alpha\kappa}$ are the fixed-J centroids and widths, which will be defined later, $E_{\rm gs}$ is the g.s. energy, η is the cutoff parameter, and N is the normalization factor corresponding to the following condition: $\int_{-\infty}^{+\infty} G(x,\sigma)\, dx = 1$. In this work we treat η as a free parameter. From previous works (see, for example, Ref. [22]) we know that the cutoff parameter is $\eta \sim 3$. We can slightly variate the value of η to achieve a better description of the nuclear level density, see Fig. 3.

The J-dependent moments method provides a good description of the exact J-dependent shell-model level density. Figure 1 presents the results for ^{28}Si in the sd shell for different values of spin J and positive parity. Figures 4 and 5 present results for ^{52}Fe and ^{52}Cr nuclei in the pf shell. Similar results were obtained for the density of states using the general moments method (see examples in Refs. [22,23,38]). A very important ingredient for our method is an accurate knowledge of the g.s. energy $E_{\rm gs}$. It is also important to investigate the sensitivity of the results to the the cutoff parameter η, and find optimal values for it. These issues will be discussed in more detail in Sec. IV.

Let us define now the fixed-J centroids and widths from Eq. (2). To calculate them for a two-body Hamiltonian,

$$H = \sum_i \epsilon_i a_i^\dagger a_i + \frac{1}{4}\sum_{ijkl} V_{ijkl} a_i^\dagger a_j^\dagger a_l a_k, \tag{4}$$

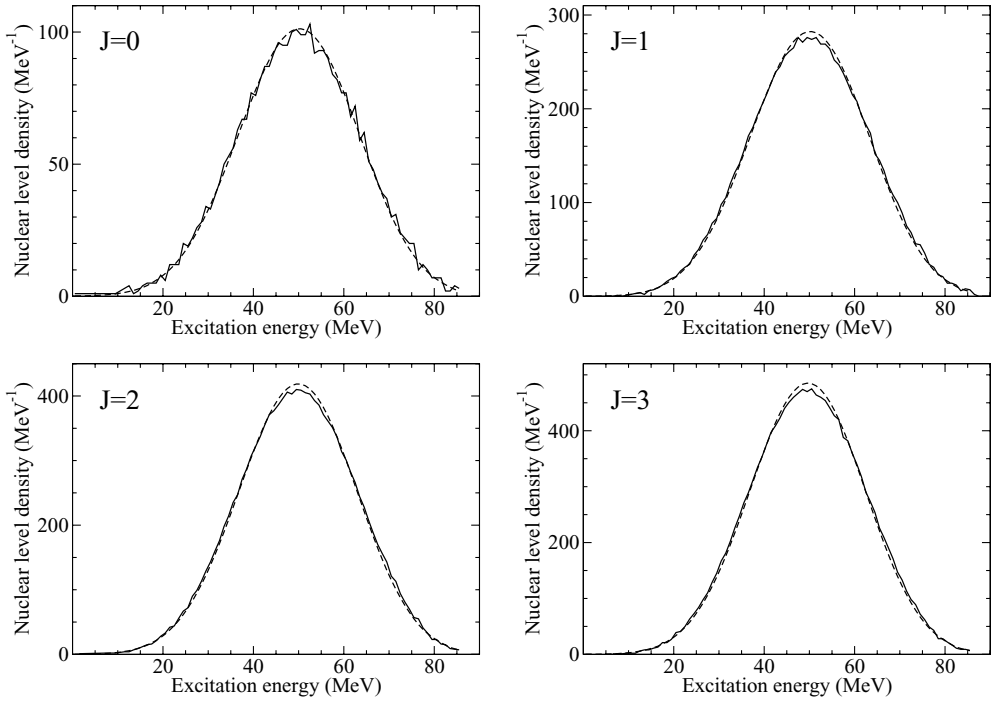

FIG. 1. ^{28}Si, parity $= +1$. Comparison of nuclear level densities between exact shell model (solid line) and moments method (dashed line). Cutoff parameter $\eta = 2.8$, interaction: USD, sd shell.

one has to calculate traces of the first and second power of this Hamiltonian, $\mathrm{Tr}[H]$ and $\mathrm{Tr}[H^2]$, for each configuration κ

$$E_{\alpha\kappa} = \langle H\rangle_{\alpha\kappa}, \tag{5}$$

$$\sigma_{\alpha\kappa} = \sqrt{\langle H^2\rangle_{\alpha\kappa} - \langle H\rangle^2_{\alpha\kappa}}, \tag{6}$$

where

$$\langle H\rangle_{\alpha\kappa} = \mathrm{Tr}^{(\alpha\kappa)}[H]/D_{\alpha\kappa}, \tag{7}$$

$$\langle H^2\rangle_{\alpha\kappa} = \mathrm{Tr}^{(\alpha\kappa)}[H^2]/D_{\alpha\kappa}. \tag{8}$$

Here the symbol of trace $\mathrm{Tr}^{(\alpha\kappa)}[\cdots]$ means the sum of all diagonal matrix elements, as $\sum\langle\nu, J|\cdots|\nu, J\rangle$, over all many-body states $|\nu, J\rangle$ belonging to the given configuration κ and having a certain set of quantum numbers α, including spin J. Technically, it is more convenient to derive these traces in a basis with a fixed spin projection $|\nu, M_z\rangle$, $\mathrm{Tr}^{(M_z)}[\cdots]$, rather than in the basis with fixed total spin $|\nu, J\rangle$, $\mathrm{Tr}^{(J)}[\cdots]$. J traces can be easily expressed through the M_z traces, given the spherical symmetry of the Hamiltonian

$$\mathrm{Tr}^{(J)}[\cdots] = \mathrm{Tr}^{(M_z)}[\cdots]|_{M_z=J} - \mathrm{Tr}^{(M_z)}[\cdots]|_{M_z=J+1}. \tag{9}$$

For simplicity, in Eq. (9) we omitted all quantum numbers, except the projection M_z and the total spin J.

Hereafter we use the label α to denote a set of quantum numbers that includes either the fixed M_z or the fixed J, keeping in mind that Eq. (9) can always connect them. In every important case we will point out which set of quantum numbers was used. Following the approach of Ref. [39] (a similar method can be found in Ref. [40]), we obtain the following expressions for the traces from Eqs. (7) and (8):

$$\mathrm{Tr}^{(\alpha\kappa)}[H] = \sum_i \epsilon_i D^{[i]}_{\alpha\kappa} + \sum_{i<j} V_{ijij} D^{[ij]}_{\alpha\kappa}, \tag{10}$$

$$\begin{aligned}\mathrm{Tr}^{(\alpha\kappa)}[H^2] &= \sum_i \epsilon_i^2 D^{[i]}_{\alpha\kappa} + \sum_{i<j}\left[2\epsilon_i\epsilon_j + 2(\epsilon_i+\epsilon_j)V_{ijij} + \sum_{q<l} V^2_{ijql}\right] D^{[ij]}_{\alpha\kappa} \\ &+ \sum_{(i<l)\neq l}\left[\sum_q \left(2V_{liiq}V_{ljjq} - V^2_{ijql}\right) + 2\epsilon_l V_{ijij}\right] D^{[ijl]}_{\alpha\kappa} \\ &+ \sum_{(i<j)\neq(q<l)} \left[V^2_{ijql} + V_{ijij}V_{qlql} - 4V_{qiil}V_{qjjl}\right] D^{[ijql]}_{\alpha\kappa},\end{aligned} \tag{11}$$

where i, j, l, and q are single-particle states with certain spin projections and possible occupation numbers equal to 0 or 1. Notice that the single-particle orbitals we used to define the configurations in Eq. (1), can host all particles with all possible spin projections corresponding to the orbital's spin. $D^{[i]}_{\alpha\kappa} = \mathrm{Tr}^{(\alpha\kappa)}[a^\dagger_i a_i]$ can be interpreted as a number of many-body states with fixed projection M_z (if we consider M_z traces) and the single-particle state i occupied, which can be constructed for the configuration κ, $D^{[ij]}_{\alpha\kappa} = \mathrm{Tr}^{(\alpha\kappa)}[a^\dagger_i a^\dagger_j a_j a_i]$, $D^{[ijq]}_{\alpha\kappa} = \mathrm{Tr}^{(\alpha\kappa)}[a^\dagger_i a^\dagger_j a^\dagger_q a_q a_j a_i]$, and so on. These D structures were called propagation functions in Ref. [39]. For completeness, we repeat here the recipe used to calculate them. One can show [39] that

$$D^{[r_1 r_2\cdots r_s]}_{\alpha\kappa} = \sum_{s\leqslant t\leqslant n} (-1)^{t-s} \sum_{t_1+\cdots+t_s=t} D_{\alpha'\kappa'}, \tag{12}$$

where all t_i are integers, configuration $\kappa' = \{\kappa'_1, \kappa'_2, \ldots, \kappa'_q\}$ can be derived from the original configuration $\kappa = \{\kappa_1, \kappa_2, \ldots, \kappa_q\}$ by removing t particles corresponding to the single-particle states $r_1, r_2, \ldots, r_s$. Formal expression for the new κ' configuration can be written as follows:

$$\kappa'_j = \kappa_j - \sum_{i\ (r_i\in j)} t_i, \tag{13}$$

where the sum includes only those values of i for which the corresponding single-particle state r_i belongs to the single-particle level j. We also assume that all the occupation numbers κ'_j must be positive, which imposes certain restrictions on the possible values of the amplitudes t_i. For every new configuration κ' one can easily define new quantum numbers, $\alpha' = \{n' M'_z T'_z \pi'\}$, entering Eq. (12). Examples are the new number of particles $n' = n - t$ and the new spin projection

$$M'_z = M_z - t_1 m_{r_1} - t_2 m_{r_2} - \cdots - t_s m_{r_s}, \tag{14}$$

where m_{r_i} is the M_z projection of the single-particle state r_i. The new isospin T'_z and parity π' are defined similarly.

III. THE MOMENTS METHOD ALGORITHM IN THE PROTON-NEUTRON FORMALISM

Let us describe some technical features of the algorithm we developed for the nuclear level density calculation. First of all, we treat protons and neutrons separately, that is, the basis of many-body wave functions are represented by a product of proton and neutron parts

$$|\nu, M_z\rangle = \left|\nu_p, M^{(p)}_z\right\rangle \cdot \left|\nu_n, M^{(n)}_z\right\rangle, \tag{15}$$

where $M^{(p)}_z + M^{(n)}_z = M_z$. Thus, the wave functions (15) have fixed isospin projection T_z, but do not have a fixed isospin T. As we already mentioned, it is more convenient to use the basis of wave functions with fixed spin projection M_z, rather than one with fixed spin J.

One can gain essential advantages from such a proton-neutron separation of the basis. One of them is connected to the number of configurations that appear in the sum of Eq. (1). Naturally, the number of configurations with fixed T_z is much greater than the number of configurations with fixed isospin. The large number of configurations allows the use of many-cores computers with greater efficiency. In other words, the calculation of the sum in Eq. (1) with a larger number of configurations can be more efficiently distributed on a larger number of processors. Figure 2 presents the speedup (calculation speed gain) as a function of the number of used processors. One can see that the case with the larger number of configurations, ^{68}Se, scales better than the case with the lower number of configurations, ^{64}Ge. Up to 2000 cores the speedup is almost perfect (the dotted line presents an ideal speedup). At this point the calculation time is about 1-2 minutes and further improvement is hardly achieved.

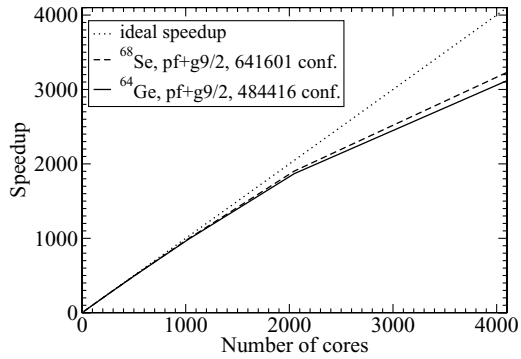

FIG. 2. Speedup is defined as T_1/T_n, where T_n is the calculation time, when n processors were used. These calculations were performed on FRANKLIN supercomputer at the National Energy Research Scientific Computing Center (NERSC) [41].

Another significant advantage of the proton-neutron formalism is the new algorithm of calculation of the dimensions $D_{\alpha\kappa}$, $D^{[i]}_{\alpha\kappa}$, $D^{[ij]}_{\alpha\kappa}$, and so on. Because of the proton-neutron separation one can calculate all proton and neutron dimensions separately. Later, the dimensions we are interested in can be easily constructed from the proton and neutron parts using the following convolution:

$$D_{M_z\kappa} = \sum_{M_z^{(p)}+M_z^{(n)}=M_z} D_{M_z^{(p)}\kappa_p} \cdot D_{M_z^{(n)}\kappa_n}, \tag{16}$$

where, instead of the whole set of quantum numbers α, only the spin projection M_z was printed out. κ_p and κ_n are the proton and neutron parts of the configuration κ. Equation (16) can be easily applied to all types of dimensions, $D^{[\cdots]}_{\alpha\ldots}$, we have shown in the formalism of Sec. II. The advantage comes from the fact that one can calculate and keep in memory all proton and neutron dimensions, $D_{M_z^{(p)}\kappa_p}$ and $D_{M_z^{(n)}\kappa_n}$, for all possible projections $M_z^{(p)}$ and $M_z^{(n)}$, and for all possible configurations κ_p and κ_n. Afterward, using Eqs. (16) and (12), one can very quickly calculate all the dimensions: $D_{\alpha\kappa}$, $D^{[i]}_{\alpha\kappa}$, $D^{[ij]}_{\alpha\kappa}$, and so on, for all M_z and J.

One more technical detail, which allows a significant speedup of the algorithm, is that using the proton-neutron separation one can avoid multiple computations of the most time-consuming structures, such as $D^{[ijql]}_{\alpha\kappa}$. Let us consider a case when all four single-particle states $\{ijql\}$ are protons. One can then use an equation similar to Eq. (16)

$$D^{[ijql]}_{M_z\kappa} = \sum_{M_z^{(p)}+M_z^{(n)}=M_z} D^{[ijql]}_{M_z^{(p)}\kappa_p} \cdot D_{M_z^{(n)}\kappa_n}. \tag{17}$$

For all configurations κ that have the same proton parts κ_p one will have to recalculate $D^{[ijql]}_{M_z^{(p)}\kappa_p}$ for each neutron configuration. Alternatively, one can calculate $D^{[ijql]}_{M_z^{(p)}\kappa_p}$ only once and store them in memory. That strategy, however, will require a large amount of storage. More efficiently, one can only store the contributions of the $D^{[ijql]}_{\alpha\kappa}$ structures to the width, Eq. (11),

TABLE I. Elapsed times of nuclear level density calculations (for all J, positive parity) with the moments method code. The calculations were done on a 16 cores machine with 2.8 GHz CPU frequency.

Element	Space	Total dim	Elapsed time (sec)
^{70}Br	$pf + g_{9/2}$	10^{15}	1.07×10^4
^{68}Se	$pf + g_{9/2}$	10^{15}	1.03×10^4
^{64}Ge	$pf + g_{9/2}$	10^{14}	0.76×10^4
^{60}Zn	pf	10^{11}	37.4
^{52}Fe	pf	10^{10}	13.6
^{28}Si	sd	10^6	0.7

that is, one can only store the following structures,

$$T_{M_z^{(p)}\kappa_p} = \sum_{(i<j)\neq(q<l)} \left[V^2_{ijql} + V_{ijij}V_{qlql} - 4V_{qiil}V_{qjjl}\right] D^{[ijql]}_{M_z^{(p)}\kappa_p}, \tag{18}$$

where all single-particle states are protons. Thus, instead of using Eq. (17) one can calculate the contribution to the width directly via the convolution

$$\mathrm{Tr}^{(\alpha\kappa)}[H^2] = \cdots + \sum_{M_z^{(p)}+M_z^{(n)}=M_z} T_{M_z^{(p)}\kappa_p} \cdot D_{M_z^{(n)}\kappa_n}, \tag{19}$$

which is very similar to Eqs. (16) and (17). As one can see the new approach avoids multiple calculations of $D^{[ijql]}_{M_z^{(p)}\kappa_p}$. Storing the structures Eq. (18) may significantly speed up the algorithm for large cases, such as ^{68}Se in $pf + g_{9/2}$ model space. The downside is that the calculation of the structures $T_{M_z^{(p)}\kappa_p}$, $T_{M_z^{(n)}\kappa_n}$ does not always scale well on a large number of cores since the number of these structures is much smaller than the total number of configurations.

Table I presents calculation times for different nuclei calculated in different shell-model spaces. The calculations were done on a 16 cores machine with 2.8 GHz CPU frequency. One core ("master") distributed all the work between the other 15 cores ("slaves"). One can emphasize here that the listed times correspond to calculations of the nuclear level densities for all J and for positive parity. For the case of ^{68}Se the largest m-scheme dimension is about 10^{15}. For each J the m-scheme dimensions vary from 10^{12} to 10^{14}, which makes direct diagonalization impossible. Using the moments method and our algorithm we are able to calculate the shapes of nuclear densities for ^{68}Se in less than three hours on a 16 cores machine. If the number of processors reaches 1000 then one needs only a few minutes to complete the calculation.

IV. RESULTS

As a first example we consider the nuclear level densities of ^{28}Si in the sd-shell model space, for which we use the USD interaction [42]. Figure 1 presents the comparison of the exact nuclear level densities of different spins (solid lines) with those obtained with the moments methods (dashed lines). Equations (1) and (2) require the knowledge of the g.s. energy E_{gs} and the cutoff parameter η. While the g.s. energy of ^{28}Si

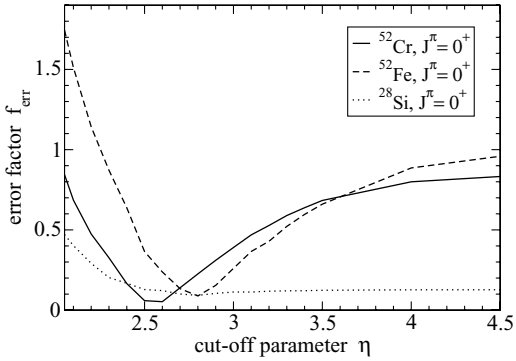

FIG. 3. Error factor $f_{\rm err}$ as function of the cutoff parameter η.

can be calculated in this case using the standard shell model, $E_{\rm gs} = -135.94$ MeV, for the value of the cutoff parameter η we only have some general idea that it should be around 3 [25,26]. In Fig. 1 by choosing $\eta = 2.8$, the moments method reproduces quite well the exact shell-model densities. To get a better description of the moments method level densities we can adjust the η parameter to optimally reproduce the exact shell-model densities. The cutoff parameter plays a similar role as that of the width in a Gaussian distribution. Indeed, if we increase the cutoff parameter then the density becomes wider and lower, while decreasing it leads to a narrowing of the density. Figure 3 helps to determine the optimal value of the cutoff parameter η. In this figure the vertical axis presents an error factor $f_{\rm err}$, which is a measure of the deviations of the calculated density $\rho_{\rm mm}$ (using the moments method) from the exact shell-model level density, $\rho_{\rm sm}$. One possible way to construct this error factor is the following [43,44]:

$$f_{\rm err} = \exp\left(\sqrt{\frac{1}{N_i}\sum_{i=1}^{N_i} \ln^2\left[\frac{\rho_{\rm mm}(E_i)}{\rho_{\rm sm}(E_i)}\right]}\right) - 1, \qquad (20)$$

where the sum over i spans an energy region, for which one wants to compare the level densities. The moments method is known to be statistically valid when the fluctuations can be described by a Gaussian orthogonal ensemble. Strictly imposing this condition may not be very practical. Therefore we consider it valid in the regime where the density is at least 5–10 levels per MeV. This condition can be used to establish a starting energy for the sum in Eq. (20). The sum should also be upper limited to excitation energies for which the $2\hbar\omega$ states are not contributing significantly. For most of the model spaces considered here this upper limit is about 10–15 MeV. Figure 3 presents the dependence of the $f_{\rm err}$ on the cutoff parameter η. It suggests that optimal values for η are in the interval 2.5–3.0, which supports our initial guess. It also indicates that there is relatively small sensitivity to this parameter in the indicated interval. Therefore, for the pf and $pf + g_{9/2}$ spaces we chose $\eta = 2.6$, the value for which the moments method level densities reproduce quite well the exact shell-model level densities. The minimum value of $f_{\rm err} = 0.1-0.2$ offers an estimated average accuracy of the moments method for the model spaces and the nuclei shown in the inset. A study of an optimal η parameters for a larger class of nuclei and model spaces will be published elsewhere [44]. One should also mention that the exact spin- and parity-dependent shell-model densities were calculated with the NuShellX code [45].

Next we present a couple of examples for the pf shell, for which we used the GXPF1A interaction [46,47]. Figures 4 and 5 present the results for ^{52}Fe ($J = 0, 1$) and for ^{52}Cr ($J = 0, 1, 2, 3$) in the pf shell, for which we have used the GXPF1A interaction [46,47]. The corresponding g.s. energies are known and the cutoff parameter was chosen to be $\eta = 2.6$. One can only compare the lowest parts of the level densities (up to 200 levels). For higher excitation energies it already becomes too difficult to calculate the exact shell-model densities because of the large number of states needed. As one can see, the moments method densities are in a very good agreement with the exact shell-model densities. Figures 4 and 5 also include results obtained by Goriely *et al.* using the Hartree-Fock-Bogoliubov (HFB) single particle energies and the combinatorial method [7,48].

We mentioned in the Introduction that one can envision using information from level densities to extract with good approximation values for the g.s. energies. Using our algorithm and the moments method one can easily calculate the nuclear level density for any nucleus that can be described in the $pf + g_{9/2}$ model space. The interaction we used for this model space was built starting with the GXPF1A interaction for the pf model space, to which G-matrix elements that describe

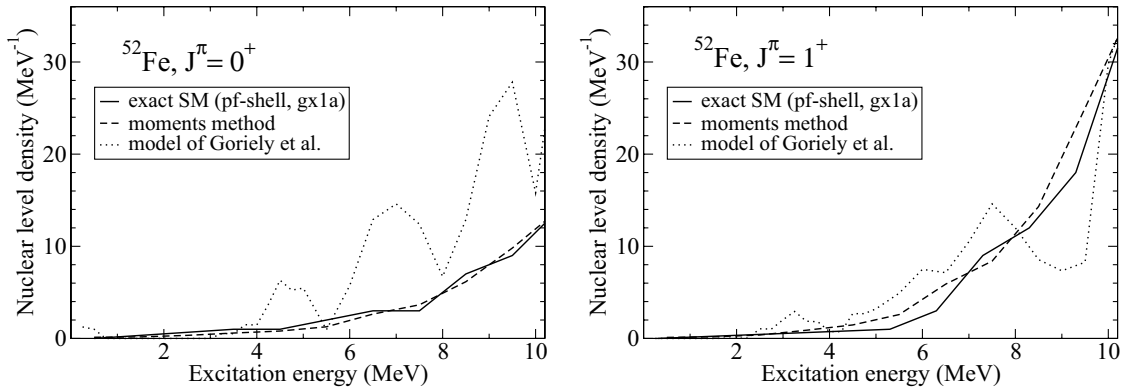

FIG. 4. ^{52}Fe, parity $= +1$. Comparison of nuclear level densities between exact shell model (solid line) and moments method (dashed line). Cutoff parameter $\eta = 2.6$, interaction: GXPF1A, pf shell.

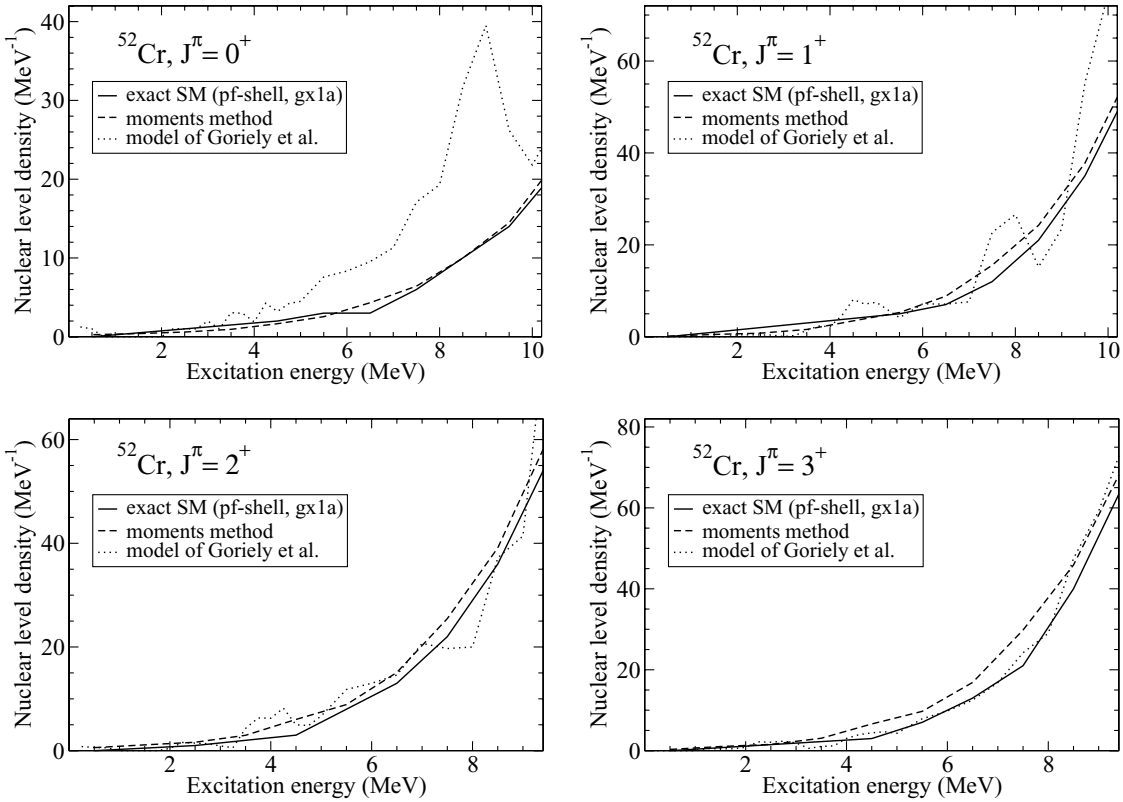

FIG. 5. ^{52}Cr, parity $= +1$. Comparison of nuclear level densities between exact shell model (solid line) and moments method (dashed line). Cutoff parameter $\eta = 2.6$, interaction: GXPF1A, pf shell.

the interaction between the pf orbits and $g_{9/2}$ orbit were added. The single particle energy for the $g_{9/2}$ orbit was fixed at -0.637 MeV. The calculation time for the worst case is more than reasonable: It takes about three hours for 16 processors and only a few minutes for 1000 processors. Figures 6 and 7 summarize the results obtained for ^{68}Se and ^{64}Ge, nuclei that are believed to be "waiting-points" in the rp-process path [49–51]. We have only presented the densities for $J = 0$, 2, and positive parity.

It is important to notice that in the pf model space the shell-model calculations of the g.s. energies can be done. For the pf shell we have the following g.s. energies: $E_{\rm gs}(pf) = -304.25$ MeV for ^{64}Ge and $E_{\rm gs}(pf) = -353.1$ MeV for ^{68}Se. Using these g.s. energies and the cutoff parameter $\eta = 2.6$, we are able to calculate the nuclear level densities according to Eqs. (1) and (2). The solid lines on Figs. 6 and 7 present the densities in the pf shell. To calculate the same level densities in the $pf + g_{9/2}$ model space we have to adjust

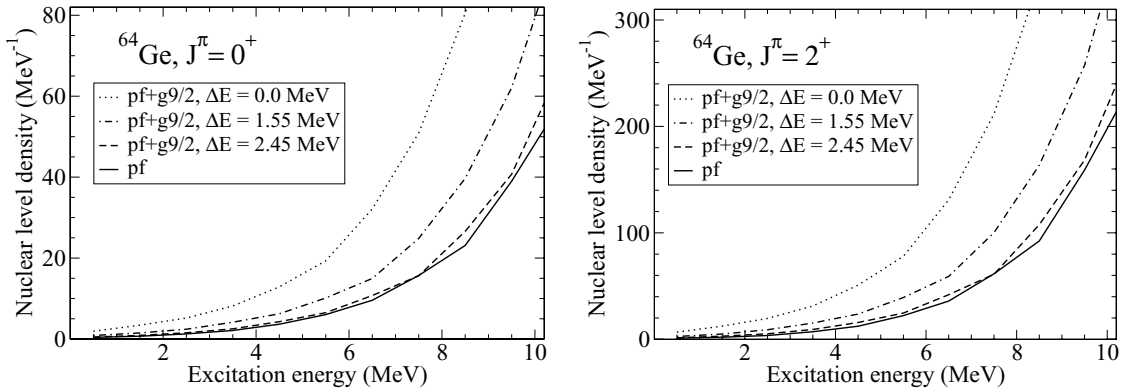

FIG. 6. ^{64}Ge nuclear level densities for $J = 0$, 2, and positive parity. Solid line presents the calculation in the pf shell with GXPF1A interaction. For this calculation we know the g.s. energy $E_{\rm gs}(pf) = -304.25$ MeV. Other three lines present calculations in the large model space, when level $g_{9/2}$ is added. The g.s. energy for these cases $E_{\rm gs}(pf + g_{9/2}) = E_{\rm gs}(pf) - \Delta E$, where ΔE is the energy shift. The cutoff parameter is $\eta = 2.6$.

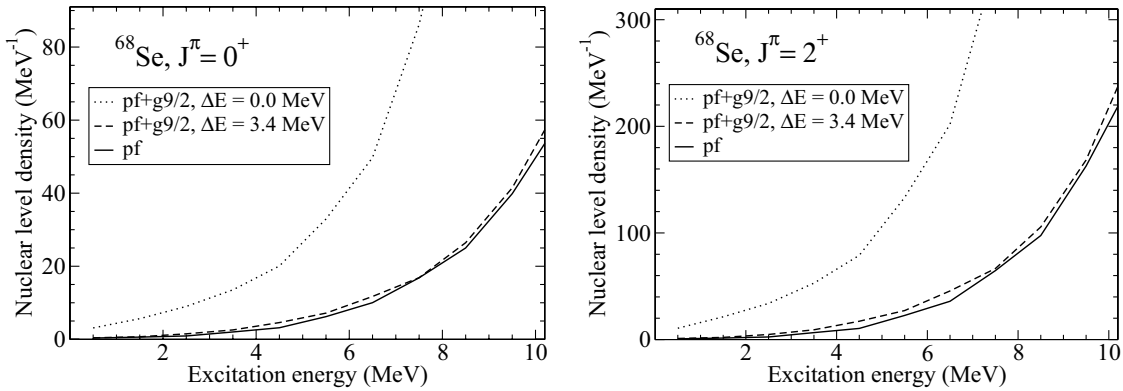

FIG. 7. ^{68}Se nuclear level densities for $J = 0$, 2, and positive parity. Solid line presents the calculation in the pf shell with GXPF1A interaction. For this calculation we know the g.s. energy $E_{\rm gs}(pf) = -353.1$ MeV. Other two lines present calculations in the large model space, when level $g_{9/2}$ is added. The g.s. energy for these cases $E_{\rm gs}(pf + g_{9/2}) = E_{\rm gs}(pf) - \Delta E$, where ΔE is the energy shift. The cutoff parameter is $\eta = 2.6$.

the g.s. energies and the cutoff parameter for this space. For the cutoff parameter we use the same value, $\eta = 2.6$. The dotted lines show the nuclear level densities if we keep the g.s. energies as they were in the pf shell. It is natural to expect only small differences between the level densities calculated in those two model spaces at low excitation energy. The difference must be compensated by the fact that the g.s. energy for the larger model space, that is, $pf + g_{9/2}$ must be lower compared to the g.s. energy for the smaller model space, that is,pf. By decreasing the g.s. energies for the $pf + g_{9/2}$ model space, one gets the dashed lines on Figs. 6 and 7. The dash-dotted lines on Fig. 6 correspond to an g.s. energy $E_{\rm gs} = -305.8$ MeV of ^{64}Ge, which was obtained by a truncated shell-model calculation in which up to six particles were excited from the $f_{7/2}$ orbits and/or into the $g_{9/2}$ orbit. The m-scheme dimension in this calculation, 13.5×10^9, is at the upper limit of the state-of-the-art shell-model calculation. As one can see, this value does not describe satisfactorily the low excitation energy level densities. To make the low-lying part of the two densities very close, one has to adjust the g.s. energies for the $pf + g_{9/2}$ model space to the following values:

$$E_{\rm gs}(pf + g_{9/2}) = -306.7 \text{ MeV} \quad \text{for} \quad ^{64}\text{Ge}, \qquad (21)$$

$$E_{\rm gs}(pf + g_{9/2}) = -356.5 \text{ MeV} \quad \text{for} \quad ^{68}\text{Se}. \qquad (22)$$

The "low-lying part of the density" should be chosen such that the excitations to the $g_{9/2}$ orbit do not give a significant contribution. For these cases we use the interval 3–6 MeV in excitation energy. We conclude that the g.s. energy adjustment of Eqs. (21) and (22) can be treated as a method of estimating the g.s. energies in larger spaces. Therefore, one can formulate now the following recipe: *ito get the g.s. energy for a nucleus in a large model space, in which the direct shell-model calculation is presently impossible, one can calculate the nuclear level densities in the large model space and in an associated smaller model space, for which the g.s. energy calculation is possible. Then, the g.s. energy for the larger model space can be estimated by demanding that the level densities in the two model spaces at low excitation energy be the same or very close.* Certainly, one should not arbitrarily select the larger model space and the associated solvable model space. What we proved here seems to be valid when adding one more single particle level to a solvable model space, such that the entire shell structure is not significantly distorted.

V. CONCLUSION AND OUTLOOK

In conclusion, we developed a very efficient algorithm to calculate the shell-model spin- and parity-dependent configurations centroids and widths, which can be used to calculate nuclear level densities. The new algorithm takes advantage of the separation of the model space in neutron and proton subspaces. This separation provides two important advantages: (i) the exponentially exploding dimensions and propagators can be calculated more efficiently in proton and neutron subspaces, and the full results can be recovered via simple convolutions; (ii) the number of configurations is significantly increased in the proton-neutron formalism, which very much improves the scalability of the algorithm on massively parallel computers. Our tests indicate almost perfect scaling for up to 4000 cores, and we are convinced that it can scale well up to tens of thousand of cores. The new algorithm is so fast that the bottleneck of the calculation is now that of the g.s. energy. That is why we cannot test our algorithm for cases that take more than 1 minute on 4000 cores.

Therefore, we investigated the possibility of using the calculated shapes of the nuclear level densities to extract the g.s. energy. We showed that by slightly incrementing the model space, and imposing the condition that the level density does not change at low expectation energy, one can reliably predict the g.s. energy, and further the full level density. This new method of extracting the shell-model g.s. energy for model spaces whose dimensions are unmanageable to direct diagonalization opens new opportunities for calculating shell-model nuclear level densities of heavier nuclei of interest for nuclear astrophysics and nuclear energy and medical physics applications. In particular, one can envision using effective interactions extracted from *ab initio* theories, such as the G matrix with core polarization, with some adjustable monopole corrections that can be tuned to describe the effect

of the correlations to nuclear level densities of heavy nuclei. This class of effective interactions is much larger than the class of pairing plus multipole interactions that Monte Carlo methods [15] can use.

The present method can be also used in more than one major harmonic oscillator shell for medium-mass nuclei to describe level densities of both parities. The center-of-mass spurious states can be eliminated in these cases using a method proposed in Ref. [27]. This method requires an extension of the present algorithm that will enforce restrictions on the classes of configurations included in the widths formula, similar to the one proposed in Ref. [26]. Work in this direction is in progress.

Our method seems to exhibit some sensitivity to the cutoff parameter η. In the cases we studied, a value of about 2.8 seems to provide very good results, but further investigations of the optimal values of this parameter are necessary. In addition, one should consider going beyond the two-moments approach for the configuration distributions. These higher moments were used in the past for the density of states. The J-dependent higher moments are more difficult to calculate, but given the computational advances we made with the first two moments, one will envision an efficient algorithm to calculate the higher moments in the near future.

ACKNOWLEDGMENTS

The authors would like to acknowledge the DOE UNEDF Grant No. DE-FC02-09ER41584 for support. M.H. acknowledges support from the NSF Grant No. PHY-0758099. The authors are also grateful to Vladimir Zelevinsky for useful discussions.

[1] W. Hauser and H. Feshbach, Phys. Rev. **87**, 366 (1952).
[2] T. Rauscher, F.-K. Thielemann, and K.-L. Kratz, Phys. Rev. C **56**, 1613 (1997).
[3] P. Möller, A. J. Sierk, T. Ichikawa, A. Iwamoto, R. Bengtsson, H. Uhrenholt, and S. Aberg, Phys. Rev. C **79**, 064304 (2009).
[4] H. A. Bethe, Phys. Rev. **50**, 332 (1936).
[5] A. G. W. Cameron, Can. J. Phys. **36**, 1040 (1958); A. Gilbert and A. G. W. Cameron, *ibid.* **43**, 14461496 (1965).
[6] T. Ericson, Nucl. Phys. **8**, 265 (1958); Adv. Phys. **9**, 425 (1960).
[7] S. Goriely, S. Hilaire, and A. J. Koning, Phys. Rev. C **78**, 064307 (2008).
[8] S. Goriely, S. Hilaire, A. J. Koning, M. Sin, and R. Capote, Phys. Rev. C **79**, 024612 (2009).
[9] H. Uhrenholt, S. Åberg, P. Möller, and T. Ichikawa, arXiv:0901.1087.
[10] W. E. Ormand, Phys. Rev. C **56**, R1678 (1997).
[11] H. Nakada and Y. Alhassid, Phys. Rev. Lett. **79**, 2939 (1997).
[12] K. Langanke, Phys. Lett. B **438**, 235 (1998).
[13] Y. Alhassid, G. F. Bertsch, S. Liu, and H. Nakada, Phys. Rev. Lett. **84**, 4313 (2000).
[14] Y. Alhassid, S. Liu, and H. Nakada, Phys. Rev. Lett. **99**, 162504 (2007).
[15] Y. Alhassid, L. Fang, and H. Nakada, Phys. Rev. Lett. **101**, 082501 (2008).
[16] E. Teran and C. W. Johnson, Phys. Rev. C **73**, 024303 (2006).
[17] E. Teran and C. W. Johnson, Phys. Rev. C **74**, 067302 (2006).
[18] V. K. B. Kota and D. Majumdar, Nucl. Phys. A **604**, 129 (1996).
[19] P. L. Huang, S. M. Grimes, and T. N. Massey, Phys. Rev. C **62**, 024002 (2000).
[20] [http://www-astro.ulb.ac.be/Html/nld.html].
[21] T. von Egidy and D. Bucurescu, Phys. Rev. C **80**, 054310 (2009).
[22] M. Horoi, M. Ghita, and V. Zelevinsky, Nucl. Phys. A **758**, 142c (2005).
[23] S. S. M. Wong, *Nuclear Statistical Spectroscopy* (Oxford University, New York, 1986).
[24] D. Mocelj, T. Rauscher, G. Martinez-Pinedo, K. Langanke, L. Pacearescu, A. Faessler, F.-K. Thielemann, and Y. Alhassid, Phys. Rev. C **75**, 045805 (2007).
[25] M. Horoi, J. Kaiser, and V. Zelevinsky, Phys. Rev. C **67**, 054309 (2003).
[26] M. Horoi, M. Ghita, and V. Zelevinsky, Phys. Rev. C **69**, 041307(R) (2004).
[27] M. Horoi and V. Zelevinsky, Phys. Rev. Lett. **98**, 262503 (2007).
[28] J. B. French and V. K. B. Kota, Phys. Rev. Lett. **51**, 2183 (1983).
[29] M. Hjorth-Jensen, T. S. Kuo, and E. Osnes, Phys. Rep. **261**, 125 (1995).
[30] M. Horoi, A. Volya, and V. Zelevinsky, Phys. Rev. Lett. **82**, 2064 (1999).
[31] M. Horoi, B. A. Brown, and V. Zelevinsky, Phys. Rev. C **65**, 027303 (2002).
[32] M. Horoi, B. A. Brown, and V. Zelevinsky, Phys. Rev. C **67**, 034303 (2003).
[33] Z. C. Gao and M. Horoi, Phys. Rev. C **79**, 014311 (2009).
[34] Z. C. Gao, M. Horoi, and Y. S. Chen, Phys. Rev. C **80**, 034325 (2009).
[35] F. S. Chang, J. B. French, and T. H. Thio, Ann. Phys. (NY) **66**, 137 (1971).
[36] K. Kar, S. Sarkar, J. M. G. Gómez, V. R. Manfredi, and L. Salasnich, Phys. Rev. C **55**, 1260 (1997).
[37] S. Choubey, K. Kar, J. M. G. Gómez, and V. R. Manfredi, Phys. Rev. C **58**, 597 (1998).
[38] T. A. Brody, J. Flores, J. B. French, P. A. Mello, A. Pandey, and S. S. M. Wong, Rev. Mod. Phys. **53**, 385 (1981).
[39] C. Jacquemin and S. Spitz, J. Phys. G **5**, L95 (1979); C. Jacquemin, Z. Phys. A **303**, 135 (1981).
[40] J. J. M. Verbaarschot and P. J. Brussaard, Phys. Lett. B **102**, 201 (1981).
[41] [www.nersc.gov].
[42] B. A. Brown and B. H. Wildenthal, Annu. Rev. Nucl. Part. Sci. **38**, 29 (1988).
[43] M. Scott and M. Horoi, Proceedings of Science (peer-reviewed), PoS(NIC-X)132 (2008), [http://pos.sissa.it/].
[44] M. Scott and M. Horoi (in preparation).
[45] W. Rae, NuShellX (2008), [http://knollhouse.org/NuShellX.aspx].
[46] M. Honma, T. Otsuka, B. A. Brown, and T. Mizusaki, Phys. Rev. C **69**, 034335 (2004).
[47] M. Honma, T. Otsuka, B. A. Brown, and T. Mizusaki, Eur. Phys. J. A **25**, 499 (2005).
[48] [http://www-astro.ulb.ac.be/Html/nld_comb.html].
[49] H. Schatz *et al.*, Phys. Rep. **294**, 167 (1998).
[50] J. A. Clark *et al.*, Phys. Rev. C **75**, 032801(R) (2007).
[51] P. Schury *et al.*, Phys. Rev. C **75**, 055801 (2007).